BULLETIN OF THE CHEMICAL SOCIETY OF JAPAN, VOL. 45, 3058—3064 (1972)

Normal Vibrations and Far-infrared Spectra of Ammonium Chloride and Ammonium Chloride-d_4 Crystals

Kunio Fukushima and Hiroko Yamamoto

Department of Chemistry, Faculty of Science, Shizuoka University, Oya, Shizuoka

(Received March 8, 1972)

The normal coordinate treatment of optically active lattice vibrations of ammonium chloride and ammonium chloride-d_4 at low temperature was made in order to elucidate the nature of the vibrations and obtain force constants in the potential in the crystals by the method of least squares. Using the constants, the optically active lattice vibrations of a crystal model for ammonium chloride and ammonium chloride-d_4 at room temperature were calculated. The far-infrared spectra obtained and the Raman and infrared spectra in literature were discussed.

Investigations of spectral change due to the phase transition in ammonium halides have been made by means of Raman and infrared spectroscopy.[1-11] Recently, by laser Raman spectroscopy, several weak Raman lines of the halides not detected in the Raman spectra obtained by use of mercury-vapor lamps as light sources, were observed. Assignments of some Raman lines to lattice vibrations were made, giving information on the lattice vibrations.[12,13] Neutron scattering expriments have given vibrational frequency data which Raman and infrared spectroscopy could not afford.[14-17] Studies on crystal structures of ammonium halides by means of X-ray, electron diffraction and neutron diffraction indicated an ordered structure for the low temperature phase.[18,19] However, no decisive conclusion has been obtained as regards the structure of the higher temperature phase.[18-21] We carried out a normal coordinate treatment of the optically active lattice vibrations of ammonium chloride and ammonium chloride-d_4 crystals in the low temperature phase in order to determine the force field in the crystals. The optically active lattice vibrations of a crystal model proposed as a model of ammonium chloride crystal at room temperature,[18] were calculated for interpretation of the infrared and Raman spectra of ammonium chloride and ammonium chloride-d_4 at room temperature.

Experimental

Ammonium chloride of the Wako Chemical Industries, Ltd. (JIS Special Grade) was recrystallized from its aqueous

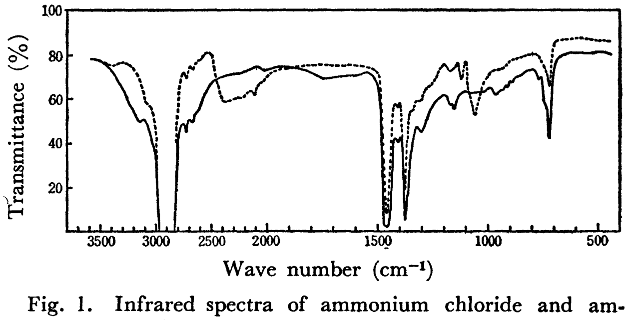

Fig. 1. Infrared spectra of ammonium chloride and ammonium chloride-d_4 in Nujol mulls.
Solid line: ammonium chloride, Dotted line: ammonium chloride-d_4.

---

[1] R. S. Krishnan, *Nature* **160**, 711 (1947).

[2] L. Couture and J. P. Mathieu, *C. R. Acad. Sci., Paris,* **266**, 1261 (1948).

[3] E. L. Wagner and D. F. Hornig, *J. Chem. Phys.*, **17**, 105(1948).

[4] E. L. Wagner and D. F. Hornig, *ibid.*, **18**, 296 (1950).

[5] D. F. Hornig, *Discuss. Farad. Soc.*, **1950**, 115.

[6] L. F. H. Bovey, *J. Chem. Phys.*, **18**, 1684 (1950).

[7] J. P. Mathieu, R. M. Aguirre, and L. Couture-Mathieu, *C. R. Acad. Sci., Paris,* **232**, 318 (1951).

[8] J. P. Mathieu and L. Couture-Mathieu, *ibid.*, **233**, 1595(1951).

[9] L. F. H. Bovey, *J. Opt. Soc. Am.*, **41**, 836 (1951).

[10] T. C. Waddington, *J. Chem. Soc.*, **1958**, 4340.

[11] C. W. Garland and N. E. Schumaker, *J. Phys. Chem. Solids*, **28**, 799 (1966).

[12] C. H. Perry and R. P. Lowndes, *J. Chem. Phys.*, **51**, 3648(1969).

[13] L. Rimai, J. Cole, and J. Parsons, "Proceedings of the Conference on Light Scattering Spectra of Solids," G. B. Wright Ed., Springer-Verlag, New York, (1969).

[14] J. J. Rush, T. I. Taylor, and W. W. Havens, Jr., *Phys. Rev. Lett.*, **5**, 507 (1960).

[15] K. Mikke and A. Kroh, Proceedings of the Symposium on Inelastic Scattering of Neutrons in Solids and Liquids (Chalk River, Canada, 10—14 September 1962); Inelastic Scattering of Neutrons in Solids and Liquids II, p. 237 (1963) (International Atomic Energy Agency, Vienna, 1963).

[16] P. S. Leung, T. I. Taylor, and W. W. Havens, Jr., *J. Chem. Phys.*, **48**, 4912 (1968).

[17] H. G. Smith, J. G. Taylor, and W. Reichard, *Phys. Rev.*, 181, 1218 (1969).

[18] G. H. Goldschmidt and D. G. Hurst, *ibid.*, **83**, 88 (1951).

[19] S. Kuwabara, *J. Phys. Soc. Jap.*, **14**, 1205 (1959).

[20] G. H. Goldschmidt and D. G. Hurst, *Phys. Rev.*, **86**, 797(1952).

[21] H. A. Levy and S. W. Petersen, *ibid.*, **86**, 766 (1952).

Table 1. Interactions taken into account in the potential and internal coordinates (R_i)

	Cell	Atom (ion)	Cell	Atom (ion)		bond length (Å)
R_{1}	(i,j,k)	1	(i,j,k)	2	N-H	1.032
R_{2}	(i,j,k)	1	(i,j,k)	3	N-H	
R_{3}	(i,j,k)	1	(i,j,k)	4	N-H	
R_{4}	(i,j,k)	1	(i,j,k)	5	N-H	
R_{5}	(i,j,k)	1	(i,j,k)	6	$N^{+}\cdot Cl^{-}$	3.308
R_{6}	(i,j,k)	1	$(i+1,j+1,k)$	6	$N^{+}\cdot Cl^{-}$	
R_{7}	(i,j,k)	1	$(i,j+1,k-1)$	6	$N^{+}\cdot Cl^{-}$	
R_{8}	(i,j,k)	1	$(i+1,j,k-1)$	6	$N^{+}\cdot Cl^{-}$	
R_{9}	(i,j,k)	1	$(i,j,k-1)$	6	$N^{+}\cdot Cl^{-}$	
R_{10}	(i,j,k)	1	$(i+1,j+1,k-1)$	6	$N^{+}\cdot Cl^{-}$	
R_{11}	(i,j,k)	1	$(i,j+1,k)$	6	$N^{+}\cdot Cl^{-}$	
R_{12}	(i,j,k)	1	$(i+1,j,k)$	6	$N^{+}\cdot Cl^{-}$	
R_{13}	(i,j,k)	2	(i,j,k)	6	$H\cdot Cl^{-}$	2.276
R_{14}	(i,j,k)	3	$(i+1,j+1,k)$	6	$H\cdot Cl^{-}$	
R_{15}	(i,j,k)	4	$(i,j+1,k-1)$	6	$H\cdot Cl^{-}$	
R_{16}	(i,j,k)	5	$(i+1,j,k-1)$	6	$H\cdot Cl^{-}$	
R_{17}	(i,j,k)	6	$(i+1,j,k)$	6	$Cl^{-}\cdot Cl^{-}$	3.820
R_{18}	(i,j,k)	6	$(i,j+1,k)$	6	$Cl^{-}\cdot Cl^{-}$	
R_{19}	(i,j,k)	6	$(i,j,k-1)$	6	$Cl^{-}\cdot Cl^{-}$	
R_{20}	(i,j,k)	6	$(i+1,j+1,k)$	6	$Cl^{-}\cdot Cl^{-}$	
R_{21}	$(i,j+1,k)$	6	$(i+1,j,k)$	6	$Cl^{-}\cdot Cl^{-}$	
R_{22}	$(i,j,k-1)$	6	$(i,j+1,k)$	6	$Cl^{-}\cdot Cl^{-}$	
R_{23}	(i,j,k)	6	$(i,j+1,k-1)$	6	$Cl^{-}\cdot Cl^{-}$	
R_{24}	$(i,j,k-1)$	6	$(i+1,j,k)$	6	$Cl^{-}\cdot Cl^{-}$	
R_{25}	$(i+1,j,k-1)$	6	(i,j,k)	6	$Cl^{-}\cdot Cl^{-}$	
R_{26}	(i,j,k)	1	$(i+1,j,k)$	1	$N^{+}\cdot N^{+}$	3.820
R_{27}	(i,j,k)	1	$(i,j+1,k)$	1	$N^{+}\cdot N^{+}$	
R_{28}	(i,j,k)	1	$(i,j,k+1)$	1	$N^{+}\cdot N^{+}$	
R_{29}	(i,j,k)	1	$(i+1,j+1,k)$	1	$N^{+}\cdot N^{+}$	
R_{30}	$(i,j+1,k)$	1	$(i+1,j,k)$	1	$N^{+}\cdot N^{+}$	
R_{31}	$(i,j,k-1)$	1	$(i,j,k+1)$	1	$N^{+}\cdot N^{+}$	
R_{32}	(i,j,k)	1	$(i,j+1,k-1)$	1	$N^{+}\cdot N^{+}$	
R_{33}	$(i,j,k-1)$	1	$(i+1,j,k)$	1	$N^{+}\cdot N^{+}$	
R_{34}	$(i+1,j,k-1)$	1	(i,j,k)	1	$N^{+}\cdot N^{+}$	
R_{35}	(i,j,k)	3	$(i+1,j,k)$	2	$H\cdot H$	2.886
R_{36}	(i,j,k)	3	$(i+1,j,k)$	4	$H\cdot H$	
R_{37}	(i,j,k)	5	$(i+1,j,k)$	2	$H\cdot H$	
R_{38}	(i,j,k)	5	$(i+1,i,k)$	4	$H\cdot H$	
R_{39}	(i,j,k)	3	$(i,j+1,k)$	2	$H\cdot H$	
R_{40}	(i,j,k)	3	$(i,j+1,k)$	5	$H\cdot H$	
R_{41}	(i,j,k)	4	$(i,j+1,k)$	2	$H\cdot H$	
R_{42}	(i,j,k)	4	$(i,j+1,k)$	5	$H\cdot H$	
R_{43}	(i,j,k)	2	$(i,j,k+1)$	4	$H\cdot H$	
R_{44}	(i,j,k)	2	$(i,j,k+1)$	5	$H\cdot H$	
R_{45}	(i,j,k)	3	$(i,j,k+1)$	4	$H\cdot H$	
R_{46}	(i,j,k)	3	$(i,j,k+1)$	5	$H\cdot H$	
R_{47}	(i,j,k)	5	$(i+1,j-1,k)$	4	$H\cdot H$	3.717
R_{48}	(i,j,k)	3	$(i+1,j+1,k)$	2	$H\cdot H$	
R_{49}	(i,j,k)	3	$(i,j+1,k+1)$	5	$H\cdot H$	
R_{50}	(i,j,k)	2	$(i,j-1,k+1)$	4	$H\cdot H$	
R_{51}	(i,j,k)	3	$(i+1,j,k+1)$	4	$H\cdot H$	
R_{52}	(i,j,k)	2	$(i-1,j,k+1)$	5	$H\cdot H$	
R_{53}	$\Delta\alpha_{213}$					
R_{54}	$\Delta\alpha_{214}$					
R_{55}	$\Delta\alpha_{215}$					
R_{56}	$\Delta\alpha_{415}$					
R_{57}	$\Delta\alpha_{314}$					
R_{58}	$\Delta\alpha_{315}$					
R_{59}	$\Delta\theta_{1}$					
R_{60}	$\Delta\theta_{2}$					
R_{61}	$\Delta\theta_{3}$					

$R_1 - R_{52}$ represent change of the corresponding atom(ion)-atom(ion) distances, respectively.

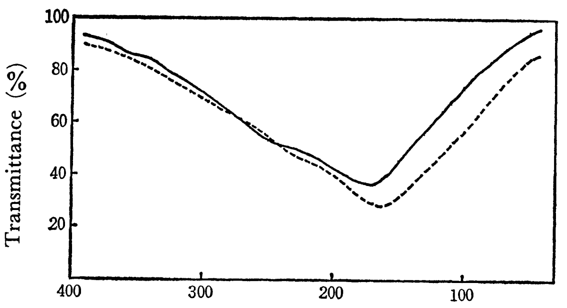

Fig. 2. Far-infrared spectra of ammonium chloride and ammonium chloride-d_4 in Nujol mulls.
Solid line: ammonium chloride, Dotted line: ammonium chloride-d_4.

solution. The deuterate was obtained by recrystallization of the ammonium chloride from its heavy water solution. Infrared spectra of Nujol mulls of the samples were measured in the region 4000—400 cm^{-1} with a Hitachi EPI-G3 spectrophotometer and in the region 400—30 cm^{-1} with a Hitachi FIS-3 Far-infrared spectrometer. The obtained spectra are shown in Figs. 1 and 2. The spectra in the region 4000—400 cm^{-1} are given in order to show the degree of deuteration by the relative intensities of N-H and N-D stretching bands.

Normal Coordinate Treatment

Normal coordinate treatments were carried out for the crystal structure of ammonium chloride at low temperature, which was confirmed by Goldschmidt and Hurst[18] (lattice parameter, a=3.820 Å; N-H=1.03 Å; space group, T_d^1; see Fig. 3) and for a crystal model[18] which might be related to the dominant structure in ammonium chloride crystal at room temperature (lattice parameter, a=7.73 Å; space group, O_h^5; see Fig. 4). Bravais lattice for the former structure is the cubic P lattice, to each lattice point of which a Bravais cell containing one NH_4Cl chemical unit belongs. That for the latter is a cubic F lattice, and the Bravais cell belonging to each lattice point contains two NH_4Cl chemical units as shown in Fig. 4. Cell repeating unit vectors are $(a_1+a_2)/2$, $(a_2+a_3)/2$, $(a_3+a_1)/2$, where a_1, a_2 and a_3 are the unit lattice vectors.

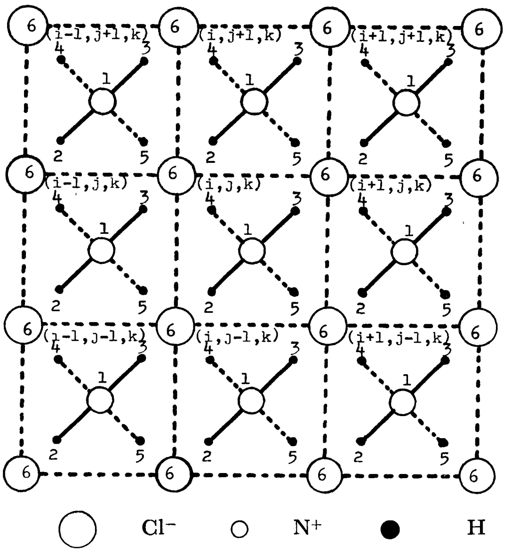

Fig. 3. A part of the structure of ammonium chloride and ammonium chloride-d_4 at low temperature (Cubic P lattice, number of chemical units per Bravais cell is one).

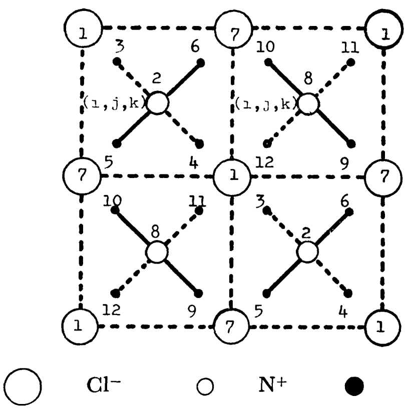

Fig. 4. A part of the unit lattice for a model of ammonium chloride and ammonium chloride-d_4 at room temperature.

Calculation of optically acitve lattice vibrations was made according to the GF matrix method developed by Shimanouchi *et al.*[22] Optically active Cartesian and internal symmetry coordinate vectors, X_{op} and R^s_{op}, are expressed as follows:

$$X_{op} = \lim_{n_1,n_2,n_3\to\infty}(n_1n_2n_3)^{-1/2}\sum_{i=0}^{n_1}\sum_{j=0}^{n_2}\sum_{k=0}^{n_3}(X)^{i,j,k}_{\mathrm{Bravais}}$$

$$R^s_{op} = \lim_{n_1,n_2,n_3\to\infty}(n_1n_2n_3)^{-1/2}\sum_{i=0}^{n_1}\sum_{j=0}^{n_2}\sum_{k=0}^{n_3}(R^s)^{i,j,k}_{\mathrm{Bravais}}$$

Here, $(\mathrm{X})^{i,j,k}_{\mathrm{Bravais}}$ and $(R^s)^{i,j,k}_{\mathrm{Bravais}}$ represent, respectively, the Cartesian displacement coordinate vector and the internal symmetry coordinate vector, which belong to the Bravais cell (i, j, k). The internal coordinate vector belonging to the Bravais cell, (i,j,k), $(\mathrm{R})^{i,j,k}_{\mathrm{Bravais}}$, and $(R^s)^{i,j,k}_{\mathrm{Bravais}}$, are shown in Tables 1 and 2, respectively. In Table 1, R_1—R_{52}, R_{53}—R_{58}, R_{59}—R_{61} are coordinate of bond stretching, angle bending and NH_4^+ rotational motions, respectively. R^s_{op} and X_{op} are related by the optically active B matrix, B^s_{op} by

$$R^s_{op} = B^s_{op}X_{op}$$

Optically active F matrix, F_{op}, is expressed by F matrix associated with the Bravais cell, (i,j,k), F_{000}, and interaction matrices between the cell and the other cells surrounding it, F_{100},F_{010},$F_{001}$$\cdots$

$$F_{op} = F_{000} + F_{100} + \tilde{F}_{100} + F_{010} + \tilde{F}_{010} + F_{001} + \tilde{F}_{001} + \cdots$$

Using X_{op}, R^s_{op} and F_{op}, optically acitve lattice vibrational frequencies were calculated by the equation

$$|M^{-1}F_{xs}-\lambda E| = 0, \quad F_{xs} = \tilde{B}^s_{op}F_{op}B^s_{op}$$

where M^{-1} is a matrix whose diagonal elements are constructed from the inverse of masses of atoms or ions in a Bravais cell.

The following potential was assumed for a Bravais cell.

$$V = V_{NH_4^+} + (1/2)\sum K(N^+\cdot Cl^-)(\Delta r_{N^+\cdot Cl^-})^2$$

---

22) T. Shimanouchi, M. Tsuboi, and T. Miyazawa, *J. Chem. Phys.*, **35**, 1597 (1961).

$$
\begin{aligned}
&+(1/2)\sum K(\mathrm{H\cdot Cl^-})(\Delta r_{\mathrm{H\cdot Cl^-}})^2\\
&+(1/2)\sum K_1(\mathrm{Cl^-\cdot Cl^-})(\Delta r_{\mathrm{Cl^-\cdot Cl^-}})_1^2\\
&+(1/2)\sum K_2(\mathrm{Cl^-\cdot Cl^-})(\Delta r_{\mathrm{Cl^-\cdot Cl^-}})_2^2\\
&+(1/2)\sum K_1(\mathrm{N^+\cdot N^+})(\Delta r_{\mathrm{N^+\cdot N^+}})_1^2\\
&+(1/2)\sum K_2(\mathrm{N^+\cdot N^+})(\Delta r_{\mathrm{N^+\cdot N^+}})_2^2\\
&+(1/2)\sum\sum_{i} K_i(\mathrm{H\cdot H})(\Delta r_{(\mathrm{H\cdot H})_i})^2\\
&+(1/2)\sum_{i=1}^{3} K_\theta \Delta(\theta_i)^2
\end{aligned}
$$

where $V_{\mathrm{NH_4^+}}$ represents the Urey-Bradley force field[23] for NH_4^+ ion, and the summation was taken over all atom(or ion)–atom(or ion) pairs of the same kind.

Table 2. Internal symmetry coordinates

A_1

$$s_i=(\sum_{j=1}^{4}R_{4(i-1)+j})/2 \qquad (i=1,2,3,4)$$
$$s_5=(\sum_{j=53}^{58}R_i)/\sqrt{6}$$
$$s_6=(\sum_{j=35}^{46}R_i)/2\sqrt{3}$$
$$s_7=(\sum_{j=1}^{3}R_{47+2(j-1)})/\sqrt{3}$$

E

$$s_1=(\sum_{j=1}^{2}2R_{53+3(j-1)}-R_{54+3(j-1)}-R_{55+3(j-1)})/2\sqrt{3}$$
$$s_2=(\sum_{j=1}^{2}R_{54+3(j-1)}-R_{55+3(j-1)})/2$$
$$s_3=(2(\sum_{j=35}^{38}R_j)-(\sum_{j=39}^{42}R_j)-(\sum_{j=43}^{46}R_j))/2\sqrt{6}$$
$$s_4=((\sum_{j=39}^{42}R_j)-(\sum_{j=43}^{46}R_j))/2\sqrt{2}$$
$$s_5=(R_{15+4i}-R_{16+4i}-R_{17+4i}-R_{18+4i})/2 \qquad (i=5,6,7)$$
$$s_8=(2R_{47}-R_{49}-R_{51})/\sqrt{6}$$
$$s_9=(R_{49}-R_{51})/\sqrt{2}$$

F_1

$$s_1=(R_{35}-R_{38}-R_{39}+R_{42})/2$$
$$s_2=(R_{36}-R_{37}+R_{44}-R_{45})/2$$
$$s_3=(R_{40}-R_{41}+R_{43}-R_{46})/2$$
$$s_4=R_{59}$$
$$s_5=R_{60}$$
$$s_6=R_{61}$$

F_2

$$s_{3i-2}=(3R_{4(i-1)+1}-R_{4(i-1)+2}+R_{4(i-1)+3}-R_{4(i-1)+4})/2\sqrt{3}$$
$$s_{3i-1}=(2R_{4(i-1)+2}-R_{4(i-1)+3}-R_{4(i-1)+4})/\sqrt{6}$$
$$s_{3i}=(R_{4(i-1)+3}-R_{4(i-1)+4})/\sqrt{2} \qquad (i=1,2,3,4)$$
$$s_i=R_{i+4} \qquad (i=13,14,15,22,23,24)$$
$$s_i=(R_{i+4}+R_{i+5})/\sqrt{2}$$
$$s_{i+1}=(R_{i+4}-R_{i+5})/\sqrt{2} \qquad (i=16,18,20,25,27,29)$$
$$s_{31}=(R_{35}-R_{38}+R_{39}-R_{42})/2$$
$$s_{32}=(R_{36}-R_{37}-R_{44}+R_{45})/2$$
$$s_{33}=(R_{40}-R_{41}-R_{43}+R_{46})/2$$
$$s_{34}=R_{48}$$
$$s_{35}=R_{50}$$
$$s_{36}=R_{52}$$
$$s_{37}=(2R_{53}-R_{54}-R_{55}-2R_{56}+R_{57}+R_{58})/2\sqrt{3}$$
$$s_{38}=(R_{54}-R_{55}-R_{57}+R_{58})/2$$
$$s_{39}=(R_{53}+R_{54}+R_{55}-R_{56}-R_{57}-R_{58})/\sqrt{6}$$

Computations were carried out at the Computer Center, the University of Tokyo, using programs BGLZ and LSMB set up in the Shimanouchi laboratory, Dept. of Chem., Faculty of Science, the University of Tokyo, and also a program made by one of the authors (K. F.).

Optically active lattice vibrations of low temperature structure were calculated for the set I force constants in Table 3. The $Cl^-\cdot Cl^-$ or $N^+\cdot N^+$ interaction potential change due to displacement Δr of a Cl^- or N^+ ion in the crystal along $Cl^-\cdot Cl^-$ or $N^+\cdot N^+$ line consists primarily of that between the ion and the nearest neighbor ions at both sides. As the interaction is electronic and proportional to r^{-1}, the potential change is expected to be proportional to $r^{-3}\cdot\Delta r^2$. Thus, $K_2(Cl^-\cdot Cl^-)$ and $K_2(N^+\cdot N^+)$ were calculated from $K_1(Cl^-\cdot Cl^-)$ and $K_1(N^+\cdot N^+)$, assuming that the $Cl^-\cdot Cl^-$ and the $N^+\cdot N^+$ force constants are proportional to r^{-3}. Using the observed frequencies in Table 4, the set of force constants were revised to set II force constants by the method of least squares.[24] Of the force constants, $K_1(Cl^-\cdot Cl^-)$, $K_2(Cl^-\cdot Cl^-)$, $K_1(N^+\cdot N^+)$ and $K_2(N^+\cdot N^+)$ were not adjusted since the optically active lattice vibrations do not change by them. By use of the set II force constants except for K_i(H·H) and K_θ, optically active lattice vibrations of the model for the structure of ammonium chloride at room temperature were calculated. The atom(or ion)-atom(or ion) interactions taken into account in the calculation are shown in Table 5. K_i(H·H) force constants for H.H length greater than 3 Å were assumed to be zero and that for 2.67_6 Å was set to 0.008 on the basis of the K_i(H·H) values in the set II and the H·H force constant values.[25] It was found by obtaining

Table 3. Force constants (in mdyn/Å)

	Set I	Set II	
K(N–H)	5.260[a]	5.193	
H(H–N–H)	0.533[a]	0.502	
F(H–N–H)	0.057[a]	0.085	
$\kappa(NH_4^+)$	−0.057[a]	−0.070	mdyn Å
$K(N^+\cdot Cl^-)$	0.067[b]	0.068	
$K(H\cdot Cl^-)$	0.067[c]	0.049	
$K_1(Cl^-\cdot Cl^-)$	0.068[c]	0.068	
$K_2(Cl^-\cdot Cl^-)$	0.024[d]	0.024	
$K_1(N^+\cdot N^+)$	0.044[e]	0.044	
$K_2(N^+\cdot N^+)$	0.016[d]	0.016	
K_1(H·H)	0.005[f]	0.005	
K_2(H·H)	0.000[f]	0.000	
K_θ	0.013[d]	0.013	mdyn Å

a) Ref. 29. b) These were determined to fit the observed frequencies, fixing other force constants. c) Ref. 26. d) These force constants were determined from $K_1(Cl^-\cdot Cl^-)$ and $K_1(N^+\cdot N^+)$, assuming that they are proportional to r^{-3}, where r represents interatomic distance. e) Ref. 22. f) Ref. 25.

---

23) T. Shimanouchi, *ibid.*, **17**, 245 (1949).

24) D. E. Mann, T. Shimanouchi, J. H. Meal, and L. Fano, *ibid.*, **27**, 43 (1957).

25) I. Harada and T. Shimanouchi, *ibid.*, **46**, 2708 (1967).

26) K. Fukushima and H. Kataiwa, This Bulletin, **43**, 690 (1970).

TABLE 4. CALCULATED AND OBSERVED FRFQUENCIES AND DOMINANT POTENTIAL ENERGY DISTRIBUTION TERMS

		Species	$\nu_{\rm obs.}$	$\nu_{\rm calc.}$	δ	p. e. d.
NH_4Cl	ν_1	A_1	3038$^{\rm a)}$	3068	+1.0	$s_1(99)$
	ν_2	E	1720$^{\rm a)}$	1724	+0.2	$s_1, s_2(98)$
	ν_3	F_1	390$^{\rm b)}$	390	0.0	$s_1, s_2, s_3(20)$; $s_4, s_5, s_6(80)$
	ν_4	F_2	3126$^{\rm c)}$	3138	+0.4	$s_1, s_2, s_3(100)$
	ν_5		1403$^{\rm c)}$	1410	+0.5	$s_{37}, s_{38}, s_{39}(100)$
	ν_6		185$^{\rm d)}$	187	+1.1	$s_4, s_5, s_6(37)$; $s_7, s_8, s_9(37)$ $s_{10}, s_{11}, s_{12}(26)$
ND_4Cl	ν_1	A_1	2215$^{\rm a)}$	2170	−2.0	$s_1(99)$
	ν_2	E	1225$^{\rm a)}$	1220	−0.4	$s_1, s_2(98)$
	ν_3	F_1		276		$s_1, s_2, s_3(20)$; $s_4, s_5, s_6(80)$
	ν_4	F_2	2336$^{\rm c)}$	2320	−0.7	$s_1, s_2, s_3(98)$
	ν_5		1067$^{\rm c)}$	1057	−0.9	$s_{37}, s_{38}, s_{39}(98)$
	ν_6		177$^{\rm d)}$	175	−1.1	$s_4, s_5, s_6(37)$; $s_7, s_8, s_9(37)$ $s_{10}, s_{11}, s_{12}(26)$

$\delta = 100(\nu_{\rm calc} - \nu_{\rm obs})/\nu_{\rm obs}$ a) Ref. 13. b) Ref. 9. c) Ref. 4. d) Ref. 12. p. e. d.: potential energy distributions (%)

TABLE 5. THE INTERACTIONS BETWEEN m-TH ATOM (OR ION) OF (i, j, k) CELL AND n-TH ATOM (OR ION) OF (i', j', k') CELL

m	(i', j', k')	n
2(N$^+$)	(i, j, k)	3(H), 4(H), 5(H), 6(H), 1(Cl$^-$), 7(Cl$^-$), 8(N$^+$)
3(H)		1(C$^-$)
1(Cl$^-$)		7(Cl$^-$)
6(H)		10(H), 12(H)
2(N$^+$)	$(i+1, j-1, k)$	1(Cl$^-$), 2(N$^+$)
4(H)		1(Cl$^-$), 3(H)
1(Cl$^-$)		1(Cl$^-$)
2(N$^+$)	$(i, j-1, k)$	2(N$^+$), 7(Cl$^-$)
1(Cl$^-$)		7(Cl$^-$)
7(Cl$^-$)		7(Cl$^-$)
4(H)		10(H), 11(H)
5(H)		6(H)
2(N$^+$)	$(i, j, k-1)$	7(Cl$^-$)
1(Cl$^-$)		7(Cl$^-$)
7(Cl$^-$)		7(Cl$^-$)
5(H)		11(H), 12(H)
2(N$^+$)	$(i+1, j, k-1)$	1(Cl$^-$)
6(H)		1(Cl$^-$)
1(Cl$^-$)		1(Cl$^-$)
2(N$^+$)	$(i+1, j-1, k-1)$	7(Cl$^-$), 1(Cl$^-$)
5(H)		1(Cl$^-$)
1(Cl$^-$)		1(Cl$^-$)
2(N$^+$)	$(i-1, j+1, k)$	8(N$^+$), 2(N$^+$)
3(H)		4(H), 9(H), 12(H)
2(N$^+$)	$(i, j+1, k)$	2(N$^+$)
6(H)		5(H)
2(N$^+$)	$(i-1, j, k+1)$	8(N$^+$), 2(N$^+$)
3(H)		9(H), 10(H)
5(H)	$(i-1, j, k)$	9(H), 11(H)
2(N$^+$)	$(i-1, j+1, k+1)$	2(N$^+$)
2(N$^+$)	$(i, j-1, k+1)$	2(N$^+$)
7(Cl$^-$)		7(Cl$^-$)
2(N$^+$)	$(i, j, k+1)$	2(N$^+$)

bond length (Å)
N-H 1.032, N$^+$·Cl$^-$ 3.350, H·Cl$^-$ 2.318, 1(Cl$^-$)·7(Cl$^-$) 3.868, 1(Cl$^-$)·1(Cl$^-$), 7(Cl$^-$)·7(Cl$^-$) 5.470, 2(N$^+$)·8(N$^+$) 3.868, 2(N$^+$)·2(N$^+$), 8(N$^+$)·8(N$^+$) 5.470, 6(H)·10(H), 4(H)·11(H), 3(H)·12(H), 5(H)·9(H), 3(H)·10(H), 5(H)·12(H) 2.676, 6(H)·12(H), 4(H)·10(H), 5(H)·11(H), 3(H)·9(H) 3.163, 4(H)·3(H), 5(H)·6(H) 3.785

Cell indices are expressed *on the basis of the basic vectors*, a_1, $(a_1+a_2)/2$, $(a_1+a_3)/2$, for convenience, and the other necessary atom(or ion)-atom(or ion) sets, which can be produced from the corresponding ones in this table by either or both of the following operations, are omitted: 1) inversion with respect to the center of 2(N$^+$)-8(N$^+$) line in (i, j, k) cell; 2) C_2 operation around any one of axes passing through both 2(N$^+$) in (i, j, k) cell and any of 8(N$^+$)'s.

calculated frequencies for various values of K_θ that only the frequencies of F_{1g} and F_{2u} vibrations (NH_4^+ rotational vibrations) change by K_θ. Therefore, K_θ value of 0.0063 mdyn. Å giving the calculated frequencies of F_{1g} vibrations fitting the observed frequencies, 345 cm^{-1}($NH_4^+Cl^-$) and 220 cm^{-1}($ND_4^+Cl^-$), was used. Calculated frequencies of low temperature structure for the set II force constants and the dominant terms of potential energy distributions, $(F_{op})_{ii}(l_{ij})^2/\lambda_j(l_{ij}$; i-th element of eigenvector for eigen value of $\lambda_j)$ are shown in Table 4. The calculated frequencies of the model of room temperature phase are shown in Table 6.

Discussion

For the crystal structures of ammonium chloride and ammonium chloride-d_4 at low temperature, which belong to the space group T_d^1, the optically active lattice vibrations are classified into nine internal vibrational modes $(1A_1+1E+2F_2)$ and six external modes $(1F_2$(translational vibrations)$+1F_1$(rotational vibrations)) by factor group analysis. Fundamental frequencies of these vibrations were selected (Table 4) on the basis of the assignments.[4,6,12,13] The F_1 vibration is both Raman and infrared inactive. The frequency value in the table is determined from combination bands by Bovey.[9] The frequency is considered to be reliable by the fact that it is in line with neutron scattering data.[14,16,17] We see from Table 4 that ν_1 is almost pure N–H(or N–D) stretching vibtations, and ν_2 and ν_5 are almost pure H–N–H(or D–N–D) bending vibrations. ν_6 vibrations of F_2 species (185 cm^{-1}, NH_4Cl; 177 cm^{-1}, ND_4Cl) are the translational lattice vibrations, in which NH_4^+ and Cl^- vibrate each other as shown in the large potential energy distribution values in Table 4, which are associated with the coordinates, s_4—s_{12}($N^+\cdot Cl^-$ stretching coordinates and $H\cdot Cl^-$ stretching coordinates). The assignment is also confirmed by the fact that shift of frequency, 185 cm^{-1}, to 177 cm^{-1} on deuteration corresponds well to the calculated shift, 187 cm^{-1} to 175 cm^{-1}. In the infrared and Raman inactive vibration ν_3, the potential energy is concentrated largely in the coordinates s_4,s_5,s_6(rotational motion coordinate of NH_4^+) and also in H·H stretching coordinates s_1,s_2,s_3. This suggests that the vibration may change its frequency on order-disorder transition. Actually, it has been found that the frequency of ν_3 vibration decreases during phase change caused by elevation of temperature.[14,16]

The set II force constants (Table 3) obtained by the method of least squares can explain the observed frequencies. The force constants except for K_i(H·H)'s and K_θ are considered to be applicable to calculations of the optically active lattice vibrations of the structure model in the room temperature phase, in which the atom(or ion)–atom(or ion) distances (Table 5) except for H·H distances are very close to those of the low temperature structure.

It has been concluded by laser Raman spectroscopic investigation[13] that among the Raman lines having frequency shifts 171 cm^{-1}, 345 cm^{-1} (NH_4Cl); 176 cm^{-1}, 220 cm^{-1} (ND_4Cl), those having frequency shifts 171 cm^{-1} and 176 cm^{-1} are due to the translational lattice vibrations corresponding to the optically active lattice vibrations (185 cm^{-1}, NH_4Cl; 177 cm^{-1}, ND_4Cl) of the low temperature phase. The Raman line with frequency shift of 345 cm^{-1} changes the shift to 220 cm^{-1} on deuteration.[13] This is clearly assigned to NH_4^+ rotational vibration. On the other hand, the infrared bands of the translational vibrations have been observed at 172 cm^{-1} (NH_4Cl) and at 166 cm^{-1} (ND_4Cl).[12] However, the bands are very broad and asymmetrical. Each band might be composed of two or more overlapped bands. Precise measurement of the purified sample of ammonium chloride in the present investigation revealed that there are at least two bands at about 240 cm^{-1} and at 170 cm^{-1}. The corresponding bands of ammonium chloride-d_4 are at about 230 cm^{-1} and at 160 cm^{-1} (Fig. 2). The results

TABLE 6. COMPARISON OF THE OBSERVED VIBRATIONAL FREQUENCIES OF NH_4Cl AND ND_4Cl AT ROOM TEMPERATURE WITH THE CALCULATED FREQUENCIES FOR A MODEL HAVING O_h^5 SYMMETRY

Observed frequencies				Calculated frequencies		Species
NH_4Cl		ND_4Cl		NH_4Cl	ND_4Cl	
IR	R	IR	R			
	3040[a]		2215[a]	3070	2172	A_{1g}
				1616	1143	E_g
	3165[a]		2350[a]	3139	2320	F_{2g}
	1400[a]		1065[a]	1358	1017	F_{2g}
	345[a]		220[a]	351	248	F_{1g}
	171[a]			171	155	F_{2g}
				3066	2169	A_{2u}
				1607	1137	E_u
3138[b]		2350[b]		3141	2322	F_{1u}
1403[b]		1066[b]		1359	1022	F_{1u}
				388	274	F_{2u}
240[c]		230[c]		255	237	F_{1u}
170[c]	171[a]	160[c]	176[a]	166	161	F_{1u}

IR: infrared absorption R: Raman scattering, a) Ref. 13. b) Ref. 4. c) Present investigation.

conclude that there are one Raman line due to translational lattice mode and two infrared bands of the corresponding modes in the Raman and infrared spectra of both ammonium chloride and ammonium chloride-d_4 at room temperature.

For the structure of ammonium chloride at room temperature three models have been proposed: (a) the free rotation model by Pauling[27] (b) the disordered model by Frenkel[28] (c) a model having the space group symmetry of O_h^5.[18,20] The possibility of (a) has been denied on experimental results. Goldschmidt and Hurst examined the validity of the models, and denied either of the models,[18] but revised their conclusion,[20] and (b) and (c) still remain as possible models. Levy and Petersen have deduced a disordered structure from their experimental results.[21] In (c), each NH_4^+ is either of two locations corresponding to its potential minima, and the nearest neighbor NH_4^+ ions surrounding one NH_4^+ are all in the same structural relation with respect to the NH_4^+. It is likely that the structural units of the model might exist as the dominant structure in (b) at higher temperature. 33 optically active lattice vibrations of (c) are classified into one A_{1g}, one A_{2u}, one E_g, one E_u, one F_{1g}, four F_{1u}, three F_{2g} and one vibrations. Among these, there are translational vibrations $(2F_{1u}+1F_{2g})$, rotational vibrations $(1F_{1g}+1F_{2u})$ and internal vibrations $(1A_{1g}+1A_{2u}+1E_g+1E_u+2F_{1u}+2F_{2g})$. The translational vibrations of F_{1u} species are infrared active and the translational vibration of F_{2g} species is Raman active. If fraction of these structural units becomes dominant in the disordered crystal, at least two infrared bands and one Raman line are expected to appear for translational vibrations. In the observed spectra, two bands which can be assigned to translational vibrations appear at 240 cm^{-1} and 170 cm^{-1} in the case of ammonium chloride, and two corresponding bands appear at 230 cm^{-1} and 160 cm^{-1} for ammonium chloride-d_4. In the Raman spectra observed by Rimai *et al.*[13] one Raman line having frequency shift of 171 cm^{-1} appears and has been assigned to a translational vibration. The rotational vibrations of NH_4^+ are both Raman and infrared inactive for the model itself. However, the corresponding vibrations of the structure in the disordered crystal, in which fraction of the structural units of the model is large, may become both Raman and infrared active because of the absence of O_h^5 symmetry in the crystal as a whole. In this case, one infrared band and one Raman line due to rotational lattice vibrations are expected to appear. Rimai *et al.* observed a Raman line having frequency shift of 345 cm^{-1}. This is reduced to 220 cm^{-1} for ammonium chloride-d_4.[13] In the infrared spectra of ammonium chloride (Fig. 2), a very weak band appears at about 360 cm^{-1} which shifts to a lower frequency on deuteration.

The calculated frequencies of the vibrations 255 cm^{-1}, 166 cm^{-1} (NH_4Cl), 237 cm^{-1}, 161 cm^{-1} (ND_4Cl) (infrared active translational vibrations) correspond to the observed frequencies of the above mentioned infrared bands (Table 6). The frequency shift expected from calculation on deuteration also corresponds to the observed shift. The calculated frequency of F_{2g} translational vibration of the model also corresponds to the observed Raman shift frequency of 171 cm^{-1} (Table 6). The results suggest that in the disordered structure of ammonium chloride in the room temperature phase, its dominant structure consists of the model units of (c).

---

[27] L. Pauling, *Phys. Rev.*, **36**, 430 (1930).

[28] J. Frenkel, *Acta Physicochimica*, **3**, 23 (1935).

[29] I. Nakagawa and S. Mizushima, This Bulletin, **28**, 589 (1955).